An Effective High Step-Up Interleaved DC-DC Converter Photovoltaic Grid Connection System

G. Lakpathi, S. Manohar Reddy, K. Lakshmi Ganesh, G. Satyanarayana

Abstract— Within the photovoltaic (PV) power generation systems in the market, the ac PV module has shown obvious growth. However, a high voltage gain converter is concentrate for the module's grid connection with dc-ac inverter. This paper proposed a converter that employs a floating active switch to isolate energy from the PV panel when the ac module is OFF; this particular design protects installers and users from electrical hazards. Without extreme duty ratios and numerous turns-ratio of a coupled inductor, this converter achieves a high step-up voltage-conversion ratio; the leakage inductor energy of the coupled inductor is efficiently recycled to the load. These features explain about module's high-efficiency performance. The detailed operating principles and steady-state analyses of continuous mode is described. A 15 volts produces from photovoltaic which is connects to high step-up dc-dc converter to produces output voltage of 170 volts. The novel proposed system is "an effective high step up interleaved dc-dc converter photovoltaic grid connection system". In this configuration consists of PV array, high step-up interleaved dc-dc converter and three-phase inverter with grid connected system. In this system, the THD value per phase voltage of three phase inverter output without filter is 1.74% with grid connection system. In this same configuration with 2nd order filter connected of three phase inverter output, the THD value reduced to 0.08%. The results are shown in Matlab/simulink 2009a.

Index Terms—AC module, coupled inductor, high step-up voltage gain, single switch, three-phase inverter, grid connection.

I. INTRODUCTION

Photovoltaic (PV) power-generation systems are becoming increasingly important and prevalent in distribution generation systems. The use of new efficient photovoltaic solar cells (PVSCs) has emerged as an alternative measure of renewable green power, energy conservation and demand-side management. Photovoltaic solar cells have initial high costs; PVSCs have not yet been a fully attractive alternative for electricity users who are able to buy cheaper electrical energy from the utility grid. However, they have been used extensively for water pumping and air conditioning in remote and isolated areas where utility power is not available or is too expensive to transport.

G. Lakpathi, Department of Electrical & Electronics Engineering, TKR college of Engineering & technology, meerpet, saroornagar , HYD.Dist., PIN-500035,A.P, India

S. ManoharReddy,Department of Electrical & Electronics Engineering, TKR college of Engineering & technology, meerpet, saroornagar, HYD.Dist., PIN-500035,A.P, India

K. Lakshmi Ganesh,MIAEME, Asst. Professor, Department of Electrical & Electronics Engineering, Vishnu Institute of Technology, vishnupur,Bhimavaram,W.G.Dist.,PIN-534202,A.P,India

G. Satyanarayana,M.Tech, PGDBM, School of Management Studies, University of Hyderabad, Hyderabad

Although PVSC prices have decreased considerably during the last years due to new developments in the film technology and manufacturing process [1], PV arrays are still widely considered as an expensive choice compared with existing utility fossil fuel generated electricity. After building such an expensive renewable energy system, the user naturally wants to operate the PV array at its highest energy conversion output by continuously utilizing the maximum available solar power of the array.

A centralized PV array is a serial connection of numerous panels to obtain higher dc-link voltage for main electricity through a dc-ac inverter [2], [30]. Unfortunately, once there is a partial shadow on some panels, the system's energy yield becomes significantly reduced [3]. An ac module is a micro inverter configured on the rear bezel of a PV panel [2]-[4]; this alternative solution not only immunizes against the yield loss by shadow effect, but also provides flexible installation options in accordance with the user's budget [5]. Many prior research works have proposed a single-stage dc-ac inverter with fewer components to fit the dimensions of the bezel of the ac module, but their efficiency levels are lower than those of conventional PV inverters. The power capacity range of a single PV panel is about 100W to 300W and the maximum power point (MPP) voltage range is from 15V to 40V, which will be the input voltage of the ac module; in cases with lower input voltage, it is difficult for the ac module to reach high efficiency [4]. However, employing a high step-up dc-dc converter in the front of the inverter improves power conversion efficiency and provides a stable dc link to the inverter.

When installing the PV generation system during daylight, for safety reasons, the ac module outputs zero voltage [5], [6]. The Fig.1 shows below the solar energy through the PV panel and micro inverter to the output terminal when the switches are OFF.
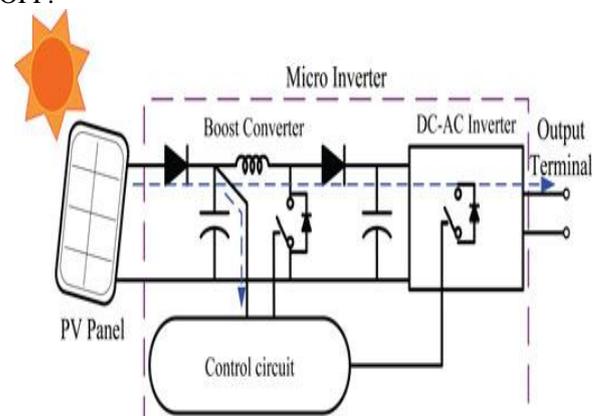

Fig.1. Potential difference on the output terminal of nonfloating switch micro inverter

When installation of the ac module is taking place, this potential difference could pose

hazards to both the worker and the facilities. A floating active switch is designed to isolate the dc current from the PV panel, for when the ac module is off-grid as well as in the no operating condition. This isolation ensures the operation of the internal components without any residential energy being transferred to the output or input terminals, which could be unsafe.

The micro inverter includes dc-dc boost converter, dc-ac inverter with control circuit as shown in Fig.1. The dc-dc converter requires large step-up conversion from the panel's low voltage to the voltage level of the application. Previous research on various converters for high step-up applications has included analyses of the switched-inductor and switched-capacitor types [7], [8]; transformer less switched-capacitor type [9], [10], [30]; the voltage-lift type [13]; the capacitor-diode voltage multiplier [14] and the boost type integrated with a coupled inductor [11], [12], these converters by increasing turns ratio of coupled inductor obtain higher voltage gain than conventional boost converter. Some converters successfully combined boost and flyback converters, since various converter combinations are developed to carry out high step-up voltage gain by using the coupled-inductor technique [15]-[20],[28],[29]. By combining active snubber auxiliary resonant circuit, synchronous rectifiers or switched capacitor based resonant circuits and so on, these techniques made active switch into zero voltage switching (ZVS) or zero current switching (ZCS) operation and improved converter efficiency[21]-[25]. However, when the leakage-inductor energy from the coupled inductor can be recycled, the voltage stress on the active switch is reduce, which means the coupled inductor employed in combination with the voltage-multiplier or voltage-lift technique successfully accomplishes the goal of higher voltage gain [2]-[13].

The proposed converter, shown in Fig. 2 is comprised of a coupled inductor $T_1$with the floating active switch S_1.

The primary winding N_1 of a coupled inductor T_1 is similar to the input inductor of the conventional boost converter and capacitor C_1 and diode D_1 receive leakage inductor energy form N_1.
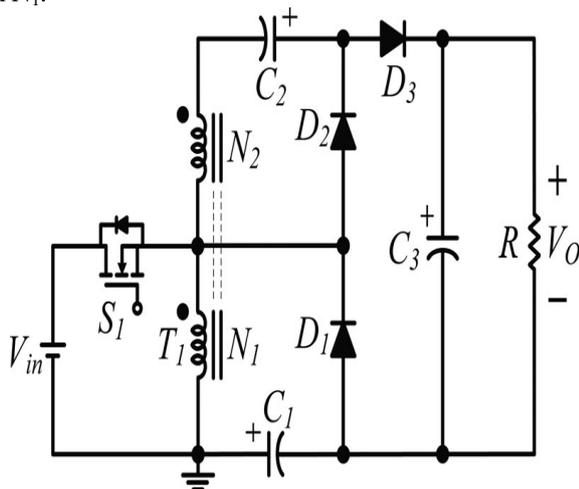

Fig.2. Circuit configuration of proposed converter

The secondary winding N_2 of coupled inductor T1 is connected with another pair of capacitors C_2 and diode D_2, which are in series with N_1 in order to further enlarge the boost voltage. The rectifier diode D_3 connects to tis output capacitor C_3. The proposed converter has several features:

1) The connection of the two pairs of inductors, capacitor and diode gives a large step-up voltage-conversion ratio
2) The leakage inductor energy of the coupled inductor can be recycled, thus increasing the efficiency and restraining the voltage stress across the active switch and
3) The floating active switch efficiently isolates the PV panel energy during no operating conditions, which enhances safety. The operating principles and steady-state analysis of the proposed converter are presented in the following section.

The novel proposed system is "an effective high step up interleaved dc-dc converter photovoltaic grid connection system". In this configuration consists of PV array, high step-up interleaved dc-dc converter and three-phase inverter with grid connected system.

II. PVA MODELING

PV arrays are built up with combined series/parallel combinations of PV solar cells, which are usually represented by a simplified equivalent circuit model such as the one given in Fig.3 and/or by an equation as in (1).
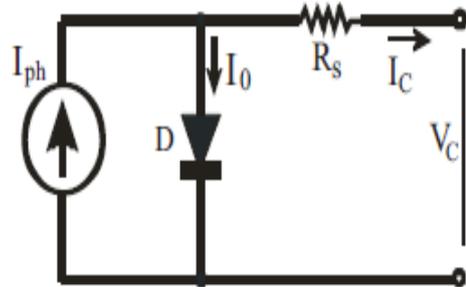

Fig.3 Simplified equivalent circuit of photovoltaic cell

The PV cell output voltage is a function of the photocurrent that mainly determined by load current depending on the solar irradiation level during the operation.

$$V_C = \frac{AkT_C}{e} ln\left(\frac{I_{Ph}+I_0-I_C}{I_0}\right) - R_S I_C \qquad (1)$$

Where the symbols are defined as follows:
e:electron charge (1.602*10^-19 C).
K: Boltzmann constant (1.38*10^-23 J/^0K).
I_C: cell output current, Amperes.
I_{ph}: photocurrent, function of irradiation level and junction Temperature (5A).
I_0: reverse saturation current of diode (0.0002A).
R_S: series resistance of cell (0.001 ohms).
T_C: reference cell operating temperature (200C).
V_C: cell output voltage, Volts.

Both k and T_C should have the same temperature unit, either Kelvin or Celsius. The curve fitting factor A is used to adjust the I-V characteristics of the cell obtained from (1) to the actual characteristics obtained by testing. Eq. (1) gives the voltage of a single solar cell which is then multiplied by the number of the cells connected in series to calculate the full array voltage. Since the array current is the sum of the currents flowing through the cells in parallel branches, the cell current I_C is obtained by dividing the array current by the number of the cells connected in parallel before being used in (1), which is only valid for a certain cell operating temperature T_C with its corresponding solar irradiation level S_C. If the temperature and solar irradiation levels change, the voltage and current outputs of the PV array will follow this

157

change. Hence, the effects of the changes in temperature and solar irradiation levels should also be included in the final PV array model. A method to include these effects in the PV array modelling is given by Buresch [32]. According to this method, for a known temperature and a known solar irradiation level, a model is obtained and then this model is modified to handle different cases of temperature and irradiation levels. Let (1) be the benchmark model for the known operating temperature T_C and known solar irradiation level S_C as given in the specification. When the ambient temperature and irradiation levels change, the cell operating temperature also changes, resulting in a new output voltage and a new photocurrent value. The solar cell operating temperature varies as a function of solar irradiation level and ambient temperature. The variable ambient temperature Ta affects the cell output voltage and cell photocurrent. These effects are represented in the model by the temperature coefficients C_{TV} and C_{TI} for cell output voltage and cell photocurrent, respectively, as:

$$C_{TV} = 1 + \beta_T(T_a - T_x) \qquad (2)$$

$$C_{TI} = 1 + \frac{\gamma_T}{S_C}((T_X - T_a) \qquad (3)$$

Where $\beta_T = .004$ and $\gamma_T = .06$ for the cell used and Ta=200C is the ambient temperature during the cell testing. This is used to obtaining the modified model of the cell for another ambient temperature T_X. Even if the ambient temperature does not change significantly during the daytime, the solar irradiation level changes depending on the amount of sunlight and clouds. A change in solar irradiation level causes a change in the cell photocurrent and operating temperature, which in turn affects the cell output voltage. If the solar irradiation level increases from S_{X1} to S_{X2}, the cell operating temperature and the photocurrent will also increases from T_{X1} to T_{X2} and from I_{ph1} to I_{ph2}, respectively. Thus the change in the operating temperature and in the photocurrent due to variation in the solar irradiation level can be expressed via two constants, C_{SV} and C_{SI}, which are the correction factors for changes in cell output voltage V_C and photocurrent I_{ph}, respectively:

$$C_{SV} = 1 + \beta_T \propto_S (S_X - S_C) \qquad (4)$$
$$C_{SI} = 1 + \frac{1}{S_C}((S_X - S_C) \qquad (5)$$

Where S_C is benchmark reference for solar irradiation level during a cell testing to obtain a modified cell model. S_X is the new level of the solar irradiation. The temperature change, ΔTC, occurs due to the change in the solar irradiation level and is obtained using

$$\Delta T_C = \propto_S (S_X - S_C) \qquad (6)$$

The constant α_S represents the slope of the change in cell operating temperature due to a change in the solar irradiation level [31] and is equal to 0.2 for the solar cells used. Using correction factors C_{TV}, C_{TI}, C_{SV} and C_{SI}, the new values of the cell output voltage V_{CX} and photocurrent I_{phx} are obtained for the new temperature T_X and solar irradiation S_X as follows:

$$V_{CX} = C_{TV} C_{SV} V_C \qquad (7)$$
$$I_{Phx} = C_{TI} C_{SI} I_{Ph} \qquad (8)$$

V_C and I_{ph} is the benchmark reference cell output voltage and reference cell photo current, respectively.

III. OPERATING PRINCIPLES OF THE PROPOSED INVERTER

The simplified circuit model of the proposed converter is shown in Fig.4. The coupled inductor T_1 is represented as a magnetizing inductor Lm, primary and secondary leakage inductors Lk1 and Lk2 and an ideal transformer. In order to simplify the circuit analysis of the proposed converter, the assumptions are made.
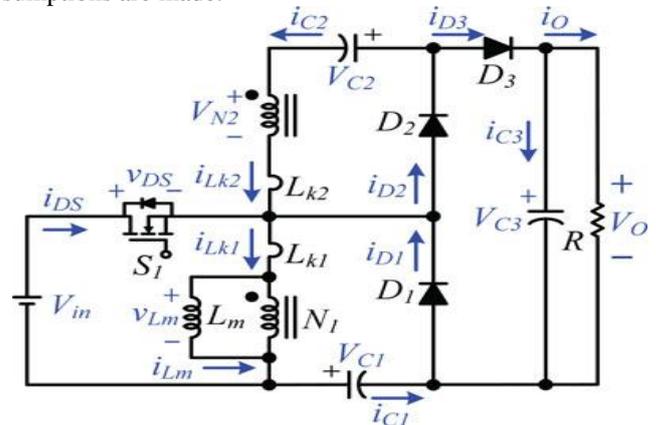

Fig.4.Polarity definitions of voltage and current in proposed converter

1) All components are ideal, except for the leakage inductance of coupled inductor T1, which is being taken under consideration. The on-state resistance RDS(ON) and all parasitic capacitances of the main switch S1 are neglected, as are the forward voltage drops of diodes D1D3.

2) The capacitors C1 C3 are sufficiently large that the voltages across them are considered to be constant.

3) The ESR (equivalent series resistance) C1 C3 and the parasitic resistance of the coupled inductor T1 are neglected.

4) The turn's ratio n of the coupled inductor T1 windings is equal to N2/N1.

The operating principle of continuous conduction mode (CCM) is presented in detail. The current waveforms of major components are given in Fig.5.

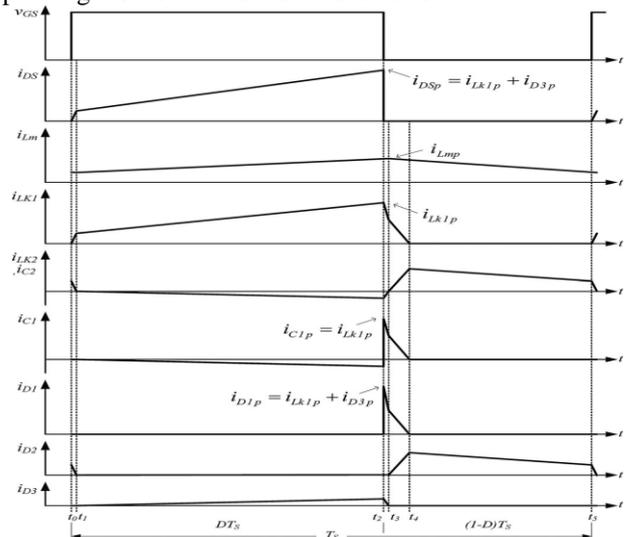There are five operating modes in a switching period. The operating modes are described as follows.

Fig.5 some typical waveforms of proposed converters at CCM operation

A. Mode I [t₀, t₁]:

In this transition interval, the magnetizing inductor L_m continuously charges capacitor C_2 through T_1 when S_1 is turned ON. The current flow path is shown in Fig. 6(a); switch S_1 and diode D_2 are conducting. The current i_{Lm} is decreasing because source voltage V_{in} crosses magnetizing inductor L_m and primary leakage inductor L_{k1}; magnetizing inductor L_m is still transferring its energy through coupled inductor T_1 to charge switched capacitor C_2, but the energy is decreasing; the charging current i_{D2} and i_{C2} are decreasing. The secondary leakage inductor current iLk2 is declining as equal to I_{Lm}/n. Once the increasing i_{Lk1} equals decreasing i_{Lm}at t = t1this mode ends.
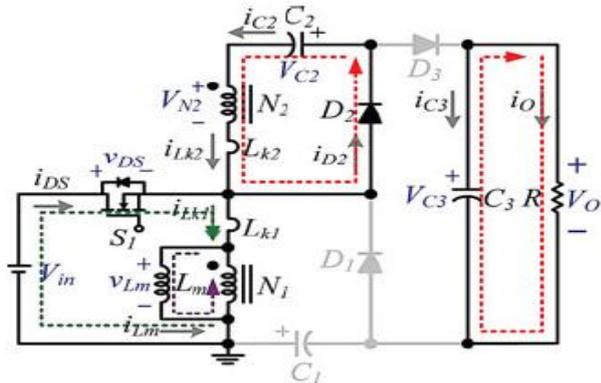

Fig. 6 (a) Current flow path of one switching period at CCM operation of ModeI:t₀~t₁.

B. Mode II [t₁,t₂]:

During this interval, source energy $V_{in}$is series connected with N_2, C_1 and C_2 to charge output capacitor C_3 and load R; meanwhile magnetizing inductor L_m is also receiving energy form V_{in}. The current flow path is shown in Fig. 6(b), where switch S_1 remains ON and only diode D_3 is conducting. The i_{Lm}, i_{Lk1} and i_{D3} are increasing because the Vin is crossing L_{k1},L_m and primary winding N_1; L_m and L_{k1} are storing energy form V_{in}; meanwhile V_{in} is also serially connected with secondary winding N_2 of coupled inductor T_1, capacitors C_1 and C_2 and then discharges their energy to capacitor C_3 and load R. The i_{in}, i_{D3} and discharging current$|i_{C1}|$ and $|i_{C2}|$ are increasing. This mode ends when switch S_1 is turned OFF at t = t₂.
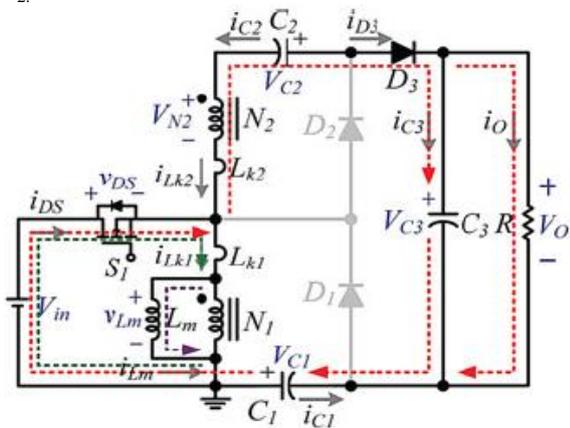

Fig. 6 (a) Current flow path of one switching period at CCM operation of ModeII:t₁~t₂

C. MODE III [T₂,T₃]:

During this transition interval, secondary leakage inductor L_{k2} keeps charging C_3 when switch S1 is OFF. The current

flow path is shown in Fig. 6(c), where only diode D_1 and D_3 are conducting. The energy stored in leakage inductor L_{k1} flows through diode D_1 to charge capacitor C_1 instantly when S_1 is OFF. Meanwhile, the energy of secondary leakage inductor L_{k2} is series connected with C_2 to charge output capacitor C_3 and the load. Because leakage inductance L_{k1} and L_{k2} are far smaller than L_m, i_{Lk2} rapidly decreases, but i_{Lm} is increasing because magnetizing inductor L_m is receiving energy form L_{k1}. Current i_{Lk2} decreases until it reaches zero; this mode ends at t=t₃.
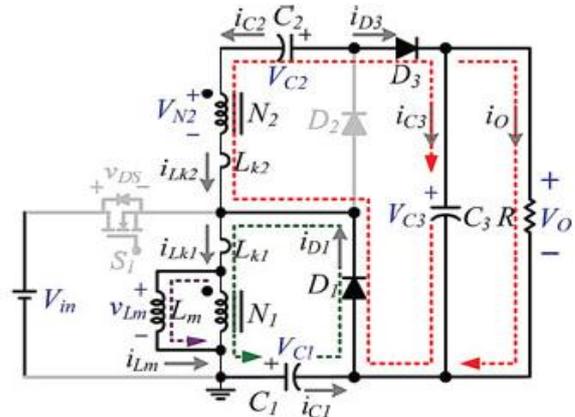

Fig. 6 (c) Current flow path of one switching period at CCM operation of ModeIII:t₂~t₃.

D. Mode IV [t₃,t₄]:

During this transition interval, the energy stored in magnetizing inductor L_m is released to C_1 and C_2 simultaneously. The current flow path is shown in Fig. 6(d). Only diodes D_1 and D_2 are conducting. Currents i_{Lk1} and i_{D1} are continually decreased because the leakage energy still flowing through diode D_1 keeps charging capacitor C_1. The L_m is delivering its energy through T_1 and D_2 to charge capacitor C_2. The energy stored in capacitor C_3 is constantly discharged to the load R. These energy transfers result in decreases in i_{Lk1} and i_{Lm} but increases in i_{Lk2}. This mode ends when current i_{Lk1} is zero, at t=t₄.
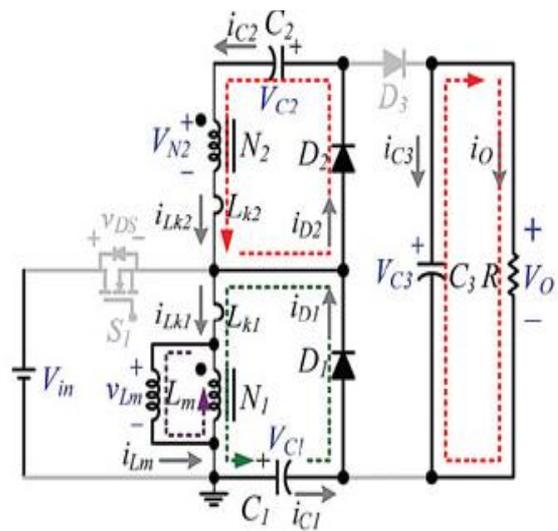

Fig. 6 (d) Current flow path of one switching period at CCM operation of ModeIV:t₃~t₄

E. Mode V [t_4, t_5]:

During this interval, only magnetizing inductor L_m is constantly releasing its energy to C_2. The current flow path is shown in Fig. 6(e), in which only diode D_2 is conducting. The i_{Lm} is decreasing due to the magnetizing inductor energy flowing through the coupled inductor T_1 to secondary winding N_2 and D_2 continues to charge capacitor C_2. The energy stored in capacitor C_3 is constantly discharged to the load R. This mode ends when switch S_1 is turned ON at the beginning of the next switching period.
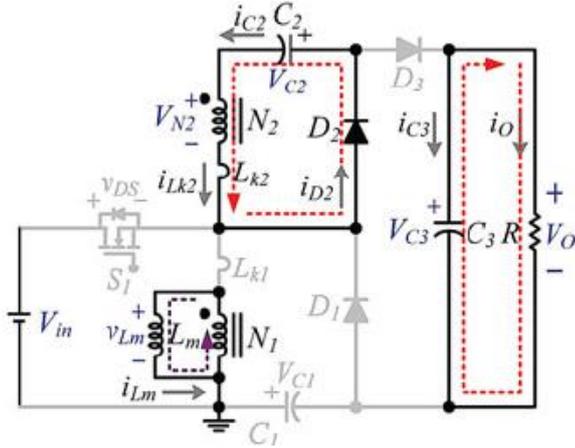

Fig. 6 (e) Current flow path of one switching period at CCM operation of ModeIV:$t_4 \sim t_5$

IV. STEADY-STATE ANALYSIS OF PROPOSED CONVERTER OF CCM OPERATION

To simplify the steady-state analysis, only modes II and IV are considered for CCM operation and the leakage inductances on the secondary and primary sides are neglected. The following equations can be written from Fig. 6(b):

$$v_{Ln} = V_{in} \qquad (9)$$

$$V_{N2} = nV_{in} \qquad (10)$$

During mode IV

$$V_{Lm} = -V_{C1} \qquad (11)$$

$$v_{N2} = -V_{C2} \qquad (12)$$

Applying a volt-second balance on the magnetizing inductor Lm yields

$$\int_0^{DT_s}(V_{in})dt + \int_{DT_s}^{T_s}(-V_{C1})dt = 0 \quad (13)$$

$$\int_0^{DT_s}(nV_{in})dt + \int_{DT_s}^{T_s}(-V_{C2})dt = 0 \quad (14)$$

From which the voltage across capacitors C_1 and C_2 are obtained as follows:

$$V_{C1} = \frac{D}{1-D}V_{in} \qquad (15)$$

$$V_{C2} = \frac{nD}{1-D}V_{in} \qquad (16)$$

During mode II, the output voltage $V_0 = V_{in} + V_{N2} + V_{C2} + V_{C1}$ becomes

$$V_0 = V_{in} + nV_{in} + \frac{nD}{1-D}V_{in} + \frac{D}{1-D}V_{in} \quad (17)$$

The DC voltage gain M_{CCM} can be found as follows:

$$M_{CCM} = \frac{V_0}{V_{in}} = \frac{1+n}{1-D} \quad (18)$$

Both [11] and [12] are employing coupled inductor topology as the boost typed converter integrating with coupled inductor; this technology is similar to the technology of the proposed converter. Fig.7 shows the plot of voltage gain M_{CCM} as function of duty ratio D of the proposed converter is compared with that of available converters [10, [11]. The chart reveals the voltage gain M_{CCM} of proposed converter is obviously higher than available converters. All of them are operating under the conditions: CCM and n=5.

During CCM operation, the voltage stresses on S1and $D_1 \sim D_3$ are given as

$$V_{DS} = V_{D1} = \frac{V_{in}}{1-D} \qquad (19)$$

$$V_{D2} = \frac{nV_{in}}{1-D} \qquad (20)$$

$$V_{D3} = \frac{1+n}{1-D}V_{in} \qquad (21)$$
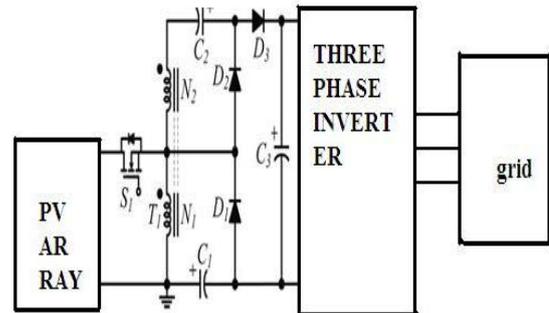
V. NEW PROPOSING SYSTEM

Fig.7. New proposing system of an effective high step up interleaved dc-dc converter photovoltaic grid connection system

In this new proposing system consists of PV array, high step-up interleaved dc-dc converter and three phase inverter with grid connection. The PV array produces 15volts voltage. This voltage is applying to high step-up interleaved dc-dc converter. The step-up voltage of their converter applied to three phase inverter. The three phase inverter output voltage is connecting to grid connection.

The three phase inverter operated with pulse generation. There are two possible patterns of conducting of the IGBT's. In one pattern each IGBT conducts for 180 degrees and in the other, each IGBT conducts for 120 degrees. But in both these patterns, conducting signals are applied and removed at 60 degrees intervals of the output voltage waveform. Therefore, both these modes require a six step bridge inverter.

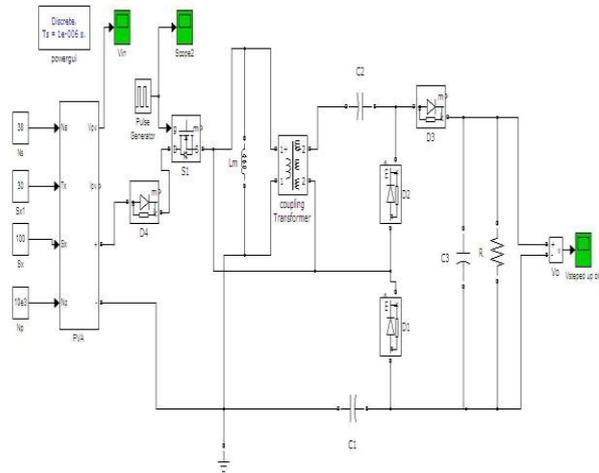## VI. SIMULATION RESULTS

A. Proposed dc-dc converter:

Fig.8. dc-dc converter with photo voltaic simulink diagram

The above figure shows simulation diagram of proposed system of dc-dc converter with photovoltaic array.
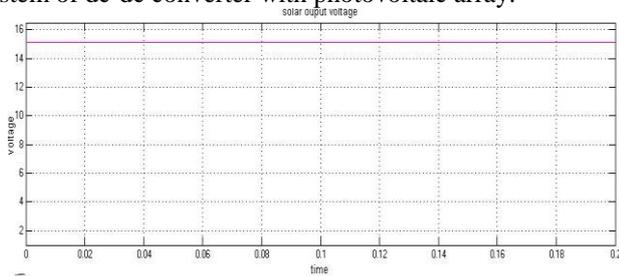

Fig.9. photovoltaic array output voltage

The above figure shows photovoltaic array produces 15volts output voltage.
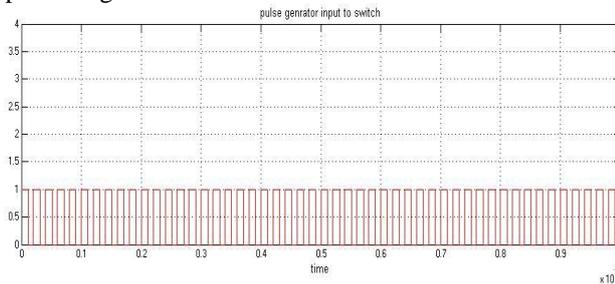

Fig.10. pulse generator input to the switch

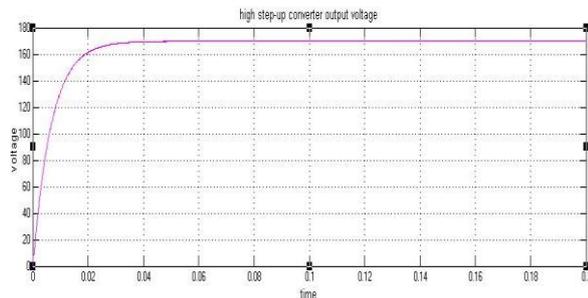The above figure shows the pulse generator output given to IGBT switch.

Fig.11. dc-dc converter output voltage

The above figure shows 170volts output voltage produced by the proposed converter.

B. New proposing system of an effective high step up interleaved dc-dc converter photovoltaic grid connection system:
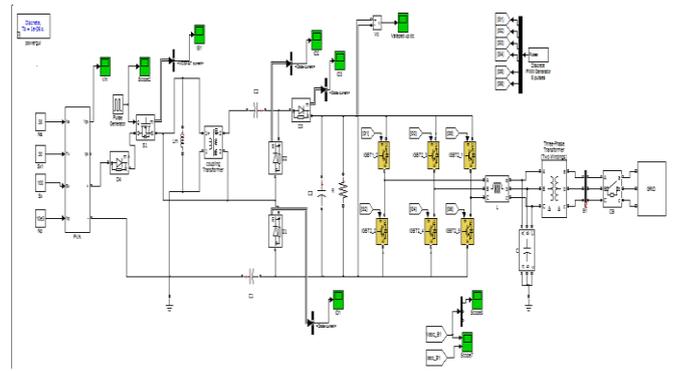

Fig.12 proposing system of an effective high step up interleaved dc-dc converter photovoltaic grid connection system

The above figure shows simulation diagram of proposing system are PV array, interleaved high step-up dc-dc converter, three phase inverter and grid connection.
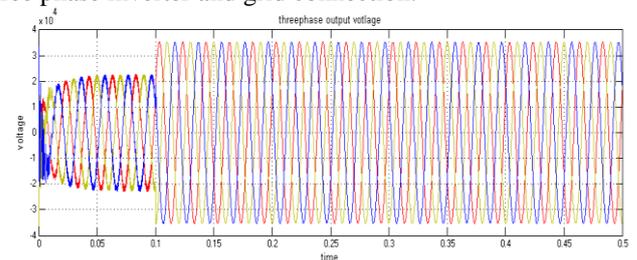

Fig.13 three phase output voltage of the three phase inverter

The above figure shows three phase output voltage produced by three phase inverter with smooth filter of inductor connection.
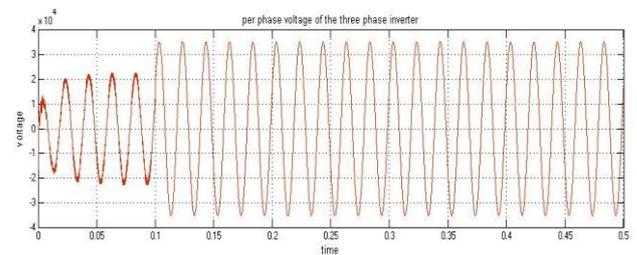

Fig.14 per phase voltage of three phase inverter

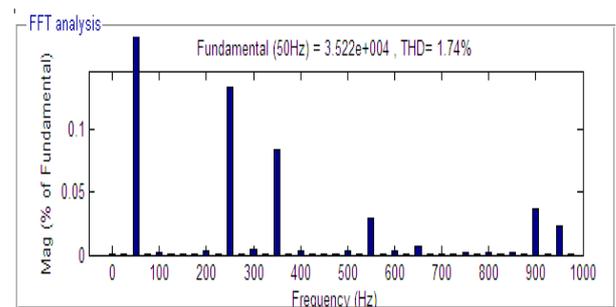The above figure shows per phase voltage of three phase inverter.

Fig.15 THD value of per phase voltage of three phase inverter without second order filter

The above figure shows THD value of 1.74% of per phase voltage of three phase inverter output voltage without second order filter connection.
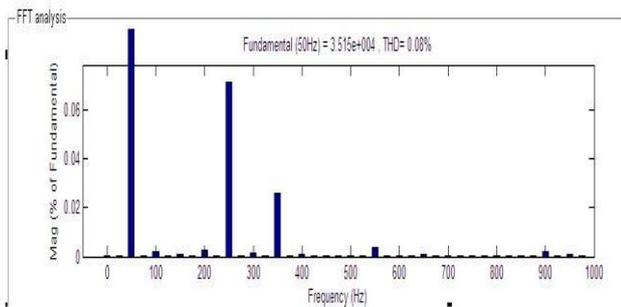
Fig.16 THD value of per phase voltage of three phase inverter with second order filter

The above figure shows THD value of 0.08% per phase voltage of three phase inverter with second order filter connection.

VII. CONCLUSIONS

In this new proposing system is "an effective high step up interleaved dc-dc converter photovoltaic grid connection system"produced three phase output voltage connected to grid connection. The THD value is 1.74% per phase voltage of three phase inverter output without second order filter connection. And THD value is 0.08% per phase voltage of three phase inverter output with second order filter connection.

The future scope is the PWM techniques used for three phase inverter are sinusoidal PWM, Third-harmonic PWM, 60 degree PWM, space vector PWM, any one PWM will use. And the other future scope is Multilevel inverters will connect to the interleaved dc-dc converter.

REFERENCES

[1] H.D.Maheshap 1998, Nagaraju e.t..V.krishna Murthy "An improved Maximum power point trcker using step-up converter with current locked loop" Renewable energy, Vol,13, issue.22,1998,pp 195-201

[2] T. Shimizu,K.Wada, and N.Nakamura, "Fly back-type single-phase utility interactive inverter with power pulsation decoupling on the dc input for an ac photovoltaic module system," *IEEE Trans. Power Electron.*, vol. 21, no. 5, pp. 1264–1272, Jan. 2006.

[3] C. Rodriguez and G. A. J. Amaratunga, "Long-lifetime power inverter for photovoltaic ac modules," *IEEE Trans. Ind. Electron.*, vol. 55, no. 7, pp. 2593–2601, Jul. 2008.

[4] S. B. Kjaer, J. K. Pedersen, and F. Blaabjerg, "A review of single-phase grid-connected inverters for photovoltaic modules," *IEEE Trans. Ind.Appl.*, vol. 41, no. 5, pp. 1292–1306, Sep./Oct. 2005.

[5] J. J. Bzura, "The ac module: An overview and update on self-containedmodular PV systems," in Proc. IEEE Power Eng. Soc. Gen. Meeting, Jul 2010, pp. 1–3.

[6] B. Jablonska, A. L. Kooijman-van Dijk, H. F. Kaan, M. van Leeuwen, G T. M. de Boer, and H. H. C. de Moor, "PV-PRIV΄E project at ECN, five years of experience with small-scale ac module PV systems," in *Proc*20th Eur. Photovoltaic Solar Energy Conf., Barcelona, Spain, Jun. 2005pp. 2728–2731.

[7] T. Umeno, K. Takahashi, F. Ueno, T. Inoue, and I. Oota, "A new approach to low ripple-noise switching converters on the basis of switched- capacitor converters," in *Proc. IEEE Int. Symp. Circuits Syst.*, Jun. 1991, pp. 1077– 1080.

[8] B. Axelrod, Y. Berkovich, and A. Ioinovici, "Switched-capacitor/ switched-inductor structures for getting transformer less hybrid dc–dc PWM converters," IEEE Trans. Circuits Syst. I, Reg. Papers, vol. 55, no. 2, pp. 687–696, Mar. 2008.

[9] B. Axelrod, Y. Berkovich, and A. Ioinovici, "Transformer less dc–dc converters with a very high dc line-to-load voltage ratio," in *Proc. IEEE Int.Symp. Circuits Syst. (ISCAS)*, 2003, vol. 3, pp. 435–438.

[10] H. Chung and Y. K. Mok, "Development of a switched-capacitor dc–dc boost converter with continuous input current waveform," *IEEE Trans.*Circuits Syst. I, Fundam. Theory Appl.,vol. 46, no. 6, pp. 756–759, Jun.1999.

[11] T. J. Liang and K. C. Tseng, "Analysis of integrated boost-fly back step-up converter," *IEE Proc. Electrical Power Appl.*, vol. 152, no. 2, pp. 217–225, Mar. 2005.

[12] Q. Zhao and F. C. Lee, "High-efficiency, high step-up dc–dc converters," *IEEE Trans. Power Electron.*, vol. 18, no. 1, pp. 65–73, Jan. 2003.

[13] M. Zhu and F. L. Luo, "Voltage-lift-type cuk converters: Topology and analysis," *IET Power Electron.*, vol. 2, no. 2, pp. 178–191, Mar. 2009.

[14] J. W. Baek, M. H. Ryoo, T. J. Kim, D. W. Yoo, and J. S. Kim, "High boost converter using voltage multiplier," in *Proc. IEEE Ind. Electron.Soc. Conf. (IECON)*, 2005, pp. 567–572.

[15] J. Xu, "Modeling and analysis of switching dc–dc converter with coupled inductor," in Proc. IEEE 1991 Int. Conf. Circuits Syst. (CICCAS), 1991,pp. 717–720.

[16] R. J.Wai, C. Y. Lin, R. Y. Duan, and Y. R. Chang, "High-efficiency dc–dc converter with high voltage gain and reduced switch stress," *IEEE Trans.Ind. Electron.*, vol. 54, no. 1, pp. 354–364, Feb. 2007.

[17] S. M. Chen, T. J. Liang, L. S. Yang, and J. F. Chen, "A cascaded high Step-up dc–dc converter with single switch for micro source applications, "*IEEE Trans. Power Electron.*, vol. 26, no. 4, pp. 1146–1153, Apr. 2011.

[18] T. J. Liang, S. M. Chen, L.S. Yang, J. F. Chen, and A. Ioinovici, "Ultra large gain step-up switched-capacitor dc–dc converter with coupled inductor for alternative sources of energy," *IEEE Trans. Circuits Syst. I*, to be published.

[19] L. S. Yang and T. J. Liang, "Analysis and implementation of a novel Bidirectional dc–dc converter," *IEEE Trans. Ind. Electron.*, vol. 59, no. 1,pp. 422–434, Jan. 2012.

[20] W. Li and X. He, "Review of non-isolated high-step-up dc/dc converters in photovoltaic grid-connected applications," *IEEE Trans. Ind. Electron.*, vol. 58, no. 4, pp. 1239–1250, Apr. 2011.

[21] S. H. Park, S. R. Park, J. S. Yu, Y. C. Jung, and C. Y. Won, "Analysis and design of a soft-switching boost converter with an HI-Bridge auxiliary resonant circuit," *IEEE Trans. Power Electron.*, vol. 25, no. 8, pp. 2142–2149, Aug. 2010.

[22] G. Yao, A. Chen, and X. He "Soft switching circuit for interleaved boost converters," *IEEE Trans. Power Electron.*, vol. 22, no. 1, pp. 80–86, Jan. 2007.

[23] Y. Park, S. Choi, W. Choi, and K. B. Lee, "Soft-switched interleaved boost converters for high step-up and high power applications," *IEEE Trans Power Electron.*, vol. 26, no. 10, pp. 2906–2914, Oct. 2011.

[24] Y.zhao, W.Li, Y.Deng, and X.He, "Analysis, design and experimentation of an isolate ZVT boost converter with coupled inductors", *IEEE Trans. Power Electron.,*vol.26, no.2, pp.541-550, Feb.2011.

[25] H.Mao,O. Abdel Rahman, and I.Batarseh, "Zero-voltage switching dc-dc converter with synchronous rectifiers," *IEEE Trans. Power Electron.,* vol.23, no.1 pp.369-378, Jan.2008.

[26] J.M. Kwon and B.H. Kwon, "High step-up active-clamp converter with input-current doubler and output-voltage doubler for fuel cell power systems," IEEE Trans. Power Electron., vol.24, no.1 pp.108-115, Jan-2009

[27] S.Dwai ad L. Parsa, "An efficient high stp-up interleaved dc-dc converter with a common active clamp," IEEE Trans. Power Electron., vol.26, no.1, pp.66-78, Jan.2011.

[28] C.Restrepo, J. Calvente ,A.Cid, A.ElAroudi, and R. Giral, " A non-inverting buck-boost dc-dc switching converter with high efficiency and wide bandwidth," IEEE Trans. Power Electron., vol.26, no.9,pp.2490-2503, sep.2011.

[29] K.B.Prk, G.W.Moon and M.J.Youn, "Nonisolated high step-up boost converter integrated with sepic converter", IEEE Trans. Power Electron., vol.25, no-9,pp.2266-2275,sep.2010.

[30] L.S.Yang, T.J.Liang and J.F.Chen, "Transformer less dc-dc converters with high step-up voltage gain, "IEEE Trans. Ind. Electron.,vol.56, no,.8,pp.3144-3153,Aug.2009.

[31] N.Pogaku, M.Prodanovic and T.C.Green, "Modeling analysis and testing of autonomous operation of an inverter-based micro grid," IEEE Trans. Power Electron., vol.22, no.2, pp.613-625, Mar.2007.

[32] M.Buresch: *photovoltaic Energy Systems Design and Installation,* McGraw-Hill, New York,1983.

An Effective High Step-Up Interleaved DC-DC Converter Photovoltaic Grid Connection System

G.Lakpathi obtained his Bachelor of Technology in Electrical and Electronics Engineering from Sri Indu college of Engineering and Technology, sheriguda, Andhra Pradesh. Present his Master of Technology in Power Electronics from TKR college of Engineering & Technology, Hyderabad, Andhra Pradesh. His areas of interests are Power Electronic Drives and Power Systems.

S.Manohar Reddy obtained his Bachelor of Technology in Electrical and Electronics Engineering from JNTUH, Andhra Pradesh. He completed Master of Engineering in Power system from OSMANIA UNIVERSITY, Hyderabad, Andhra Pradesh, India. His areas of interest are power quality and harmonic reduction. He is currently working as Assistant Professor in the Electrical and Electronics Engineering Department in TKR college of Engineering and Technology, Hyderabad, Andhra Pradesh, India.

K. Lakshmi Ganesh obtained his Bachelor of Technology in Electrical and Electronics Engineering from Anurag Engineering College, Kodad, Andhra Pradesh. He completed Master of Technology in Power Electronics from Sri Vasavi Engineering College, Andhra Pradesh,India. His areas of interest include multilevel inverters and Electrical Machines. He is currently working as Assistant Professor in the Electrical and Electronics Engineering Department in Vishnu Institute of Technology, Bhimavaram, West Godavari Dist, and Andhra Pradesh, India.

G.Satyanarayanawas born in Andhra Pradesh, India in 1988. He received his B.Tech and M.Tech degrees in Electrical & Electronics Engineering from JNTU Hyderabad and JNTU Kakinada University, Andhra Pradesh, India. His area of interests is Power Quality Improvement, FACTS Controllers, Intelligence Controllers, and Multilevel Inverters. Presently,he is pursuing PGDBM at university of Hyderabad, Hyderabad.